

Transition Metal Complexes with 2,6-Di-*tert*-butyl-*p*-quinone 1'-Phthalazinylhydrazone

S. I. Levchenkov^a, I. N. Shcherbakov^b, L. D. Popov^b, S. N. Lyubchenko^b, K. Yu. Suponitskii^c,
A. A. Tsaturyan^b, S. S. Beloborodov^b, and V. A. Kogan^b

^a Southern Scientific Center of the Russian Academy of Sciences, ul. Chekhova 41, Rostov-on-Don, 344022 Russia
e-mail: s.levchenkov@gmail.com

^b Southern Federal University, Department of Chemistry, Rostov-on-Don, Russia

^c Nesmeyanov Institute of Organoelemental Compounds, Russian Academy of Sciences, Moscow, Russia

Received November 1, 2012

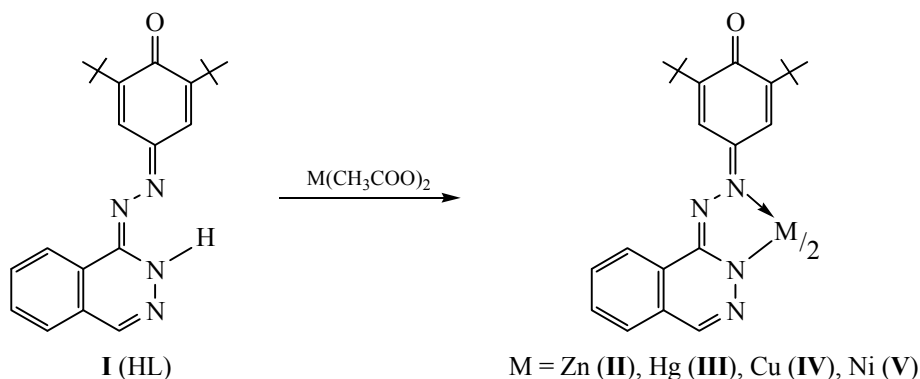
Abstract—2,6-Di-*tert*-butyl-*p*-quinone 1'-phthalazinylhydrazone (HL) was synthesized. Quantum-chemical calculations of the energy of possible tautomeric forms of the hydrazone were performed. The complexes of Zn(II), Hg(II), Ni(II), and Cu(II) of ML₂ composition were obtained and studied. The structure of the NiL₂ complex was established by XRD. It was shown by DFT-D3 calculations that the *cis*-structure of the complex is stabilized due to the interligand dispersion interaction.

DOI: 10.1134/S1070363213100216

Hydrazones of carbonyl compounds belong to one of the most popular types of ligand systems, as they easily form coordination compounds with the majority of the transition metals [1–6]. The interest in the 1-hydrazino-phthalazine (hydalazine), its derivatives, and their complexes with transition metals is due to the biological activity inherent to these compounds [6–12]. The study of the hydrazones based on hydrazine-phthalazine is stimulated by the fact that the metabolism of hydalazine includes its interaction with the

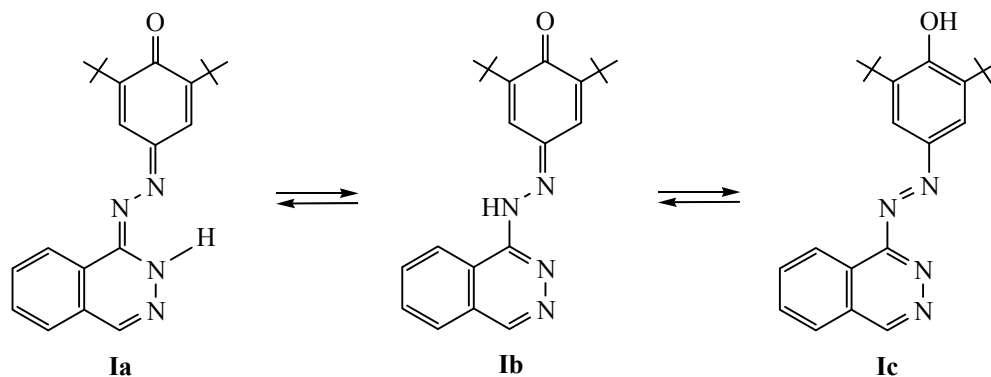
carbonyl compounds formed in the Krebs cycle [11–17]. A number of hydrazine hydrazones with some mono- and dicarbonyl compounds were described [17–20], as well as their mono- and binuclear coordination compounds with transition metals [21–30].

This paper presents the results of studies of the physical and chemical properties of 2,6-di-*tert*-butyl-*p*-quinone 1'-phthalazinylhydrazone (**I**) and the transition metal complexes **II–V** based on it.



Hydrazone **I** was identified by elemental analysis, IR and ¹H NMR spectroscopy. Compound **I** can exist in several tautomeric forms: phthalazone **Ia**, hydrazone **Ib**, and azophenol **Ic**.

The presence in the ¹H NMR spectrum of compound **I** of two proton signals from the *tert*-butyl groups indicates the presence of one of the quinoid forms, **Ia** or **Ib**. In the azophenol form **Ic** a fast (in the



NMR time scale) rotation of the phenolic moiety around the single N–C bond should be expected, that should result in the appearance in the ^1H NMR spectra of the signals of two *t*-Bu groups in the form of 18-proton singlet.

In accordance with the available data it is presumable that, as in the case of other hydrazine-phthalazine hydrazones [6, 19, 29–33], compound **I** exists primarily as phthalazonehydrazone tautomer **Ia**.

To confirm this assumption we performed quantum-chemical calculations of the electronic and steric structure of the tautomers **Ia–Ic** within the density functional theory (DFT). We used a hybrid exchange-correlation functional B3LYP [34] with the exchange part in the form proposed in the work of Becke [35], and the correlation part of the Lee–Yang–Parr [36]. The geometric structure of the molecules was initially optimized over all the natural variables without restrictions on symmetry. Minima on the potential energy surface for each structure were identified by calculation of the matrix of force constants and frequencies of normal vibrations. As the basis set we used the extended valence-split basis 6311+G(d,p).

The most stable form of the tautomers **Ia–Ic** and their relative energies are shown in Fig. 1.

According to calculations, the most stable form of compound **I** is phthalazonehydrazone tautomer **Ia**, stabilized by an intramolecular hydrogen bond. Hydrazine **Ib** and azophenol **Ic** tautomers are destabilized relative to **Ia** by 9.3 and 15.1 kcal mol $^{-1}$, respectively.

The electron absorption spectrum of the hydrazone **I** in toluene contains an absorption band at 471 nm (ϵ 34 500 L cm $^{-1}$ mol $^{-1}$). In aqueous ethanol the position of the band is almost unchanged (470 nm,

ϵ 33 500 L cm $^{-1}$ mol $^{-1}$). In an alkaline environment there is a significant red shift of the absorption band to 555 nm (ϵ 31 300 L cm $^{-1}$ mol $^{-1}$), which is associated with the formation of the deprotonated form of the hydrazone. In the acidic environment in the spectrum of the hydrazone **I** there are two absorption bands at 385 nm (ϵ 17,600 L cm $^{-1}$ mol $^{-1}$) and 399 nm (ϵ 18500 L cm $^{-1}$ mol $^{-1}$), which can be attributed to various protonated forms of the hydrazone.

Hydrazone **I** forms with Zn(II), Hg(II), Cu(II), and Ni(II) acetates the complexes of the type **II–V** of ML $_2$ composition. The disappearance of the absorption band $\nu(\text{NH})$ and low-frequency shift of the band $\nu(\text{C}=\text{N})$ in the IR spectra of complexes indicates the bidentate ligand coordination of the monodeprotonated form. In the ^1H NMR spectra of compounds **II**, **III**, and **V** there are no signals from the protons of NH-group, and there are two signals from the protons of *tert*-butyl groups, which also confirms the coordination of the ligand in monodeprotonated quinoid form.

In the electronic spectra of complexes **II–V** in toluene a red shift of the absorption band maximum is observed by 62, 56, 58, and 57 nm, respectively, as compared with its positions in the spectrum of the hydrazone **I**, due to the partial charge transfer from the anionic ligand on the metal ion.

The effective magnetic moment of the copper complex **IV** at room temperature (1.79 MB) is typical of copper(II) with a planar environment of the central ion [37, 38]. At lowering the temperature to 77.4 K the value of μ_{eff} remains practically unchanged, indicating the absence of intermolecular magnetic exchange interaction between the copper(II) ions.

According to the available data it is presumable that mercury and zinc complexes are tetrahedral, and copper and nickel complexes have planar structure.

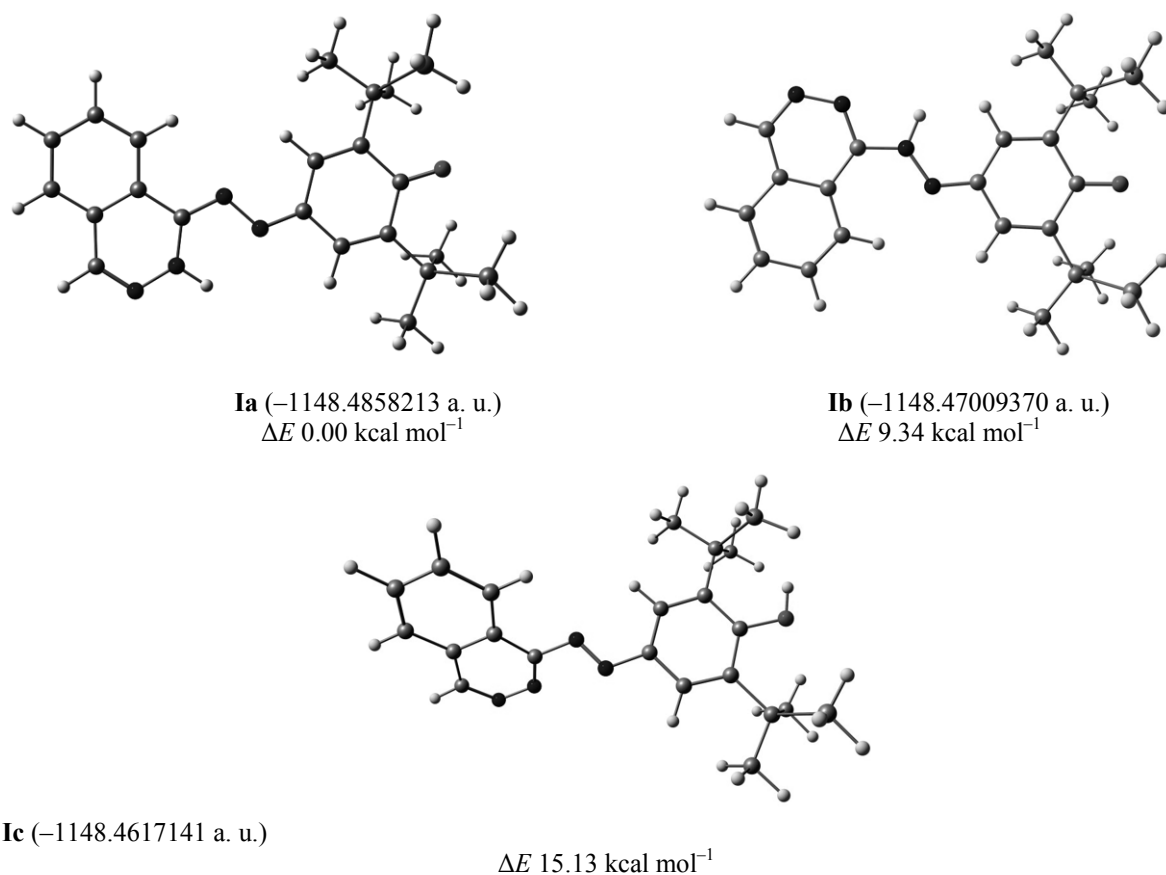


Fig. 1. The total energies (a. u.) and relative stability ΔE (kcal mol^{–1}) of tautomeric forms of the compounds **I** in a vacuum.

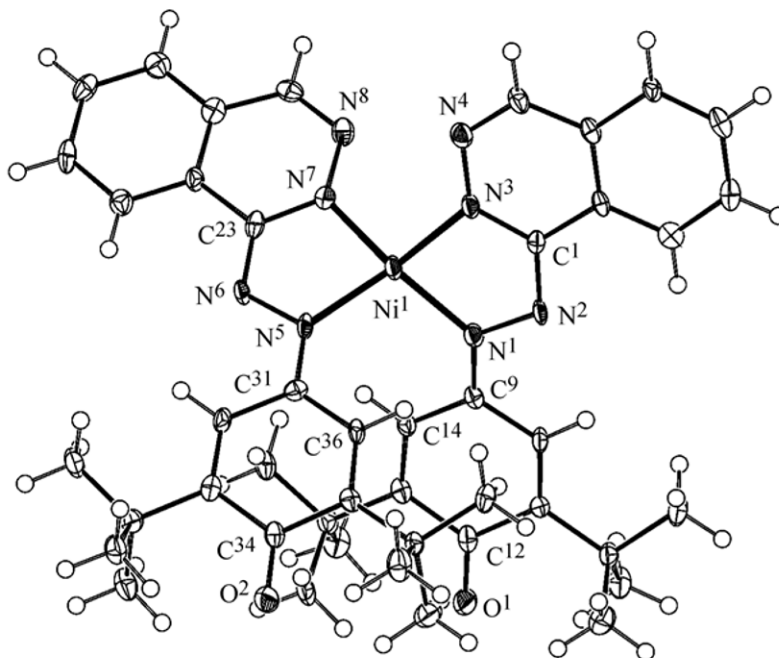


Fig. 2. The structure of complex **V**; ellipsoids of thermal vibrations are given for the 50% probability.

The latter complex can have *cis*- or *trans*-molecular structure. Given the presence in the ligand molecule of the bulky *tert*-butyl groups at the donor nitrogen atoms, it might be expected that the complexes should have *trans*-structure, in which the steric hindrance is minimal [39, 40]. However, the results of X-ray studies of the nickel complex **V** showed that the complex has an unusual *cis*-structure (Fig. 2).

Formula unit in the crystalline state is a mononuclear complex NiL_2 . Complex molecule is not symmetric, the geometric characteristics of the ligands are somewhat different from each other (Table 1). The five-membered metallocycles are essentially flat, with little distortion of the *envelope* type with nickel as the top atom. The inflection of the plane of chelate rings at the line connecting the donor nitrogen atoms in one ring ($\text{NiN}^1\text{N}^2\text{C}^1\text{N}^3$) is 4.2° , and in the second ring ($\text{NiN}^5\text{N}^6\text{C}^{23}\text{N}^7$) it is 8.9° . The two ligand molecules in general are also almost flat, the dihedral angle between the mean planes of quinonimine fragments and phthalazine rings are $-2.94(19)^\circ$ and $6.09(18)^\circ$, respectively.

The coordination polyhedron of the nickel ion in complex **V** can be described as a highly distorted square or strongly flattened tetrahedron (Fig. 2), the dihedral angle between the mean square planes of five-membered chelate rings of two ligands is $38.84(19)^\circ$. This significant tetrahedral distortion is a consequence of steric repulsion of bulky *tert*-butyl groups of the *cis*-oriented ligands and of the mutual repulsion of the lone electron pairs of nitrogen atoms N^4 and N^8 .

It is known that the tetrahedral ligand environment of nickel ion in the coordination compounds determines its high-spin state ($S = 1$), while the square-planar configuration corresponds to low-spin state ($S = 0$) [37]. It is interesting that with such a large value of the tetrahedral distortion the low-spin state of the nickel ion ($S = 0$) is realized as evidenced by its diamagnetism.

Complex **V** crystals have a very interesting structure. The molecules are packed in layers, parallel to the *aOb* crystallographic plane, so that the *t*-butyl groups are located on the surface of each layer. The areas of hydrophobic interaction are formed between the layers (Fig. 3, shaded area).

Within the layers, the molecules are connected through π - π and $\text{CH}\cdots\pi$ contacts, the shortest of which is $\text{C}^2\cdots\text{C}^{10i}$, $d = 3.289(7) \text{ \AA}$ [symmetry code (i) is $1 - x, 1 - y, -z$, by $\delta = 0.11 \text{ \AA}$ less than the sum of van der

Table 1. Selected interatomic distances and angles in the structure of complex **V** according to XRD data

| Bond | $d, \text{ \AA}$ | Angle | $\omega, \text{ deg}$ |
|-----------------------------|------------------|--------------------------------------|-----------------------|
| $\text{Ni}^1\text{--N}^7$ | 1.8624 | $\text{N}^7\text{Ni}^1\text{N}^3$ | 99.8719 |
| $\text{Ni}^1\text{--N}^3$ | 1.8594 | $\text{N}^7\text{Ni}^1\text{N}^5$ | 81.2917 |
| $\text{Ni}^1\text{--N}^5$ | 1.9244 | $\text{N}^3\text{Ni}^1\text{N}^5$ | 154.3617 |
| $\text{Ni}^1\text{--N}^1$ | 1.9454 | $\text{N}^7\text{Ni}^1\text{N}^1$ | 155.0017 |
| $\text{N}^1\text{--N}^2$ | 1.3615 | $\text{N}^3\text{Ni}^1\text{N}^1$ | 82.4418 |
| $\text{N}^1\text{--C}^9$ | 1.3316 | $\text{N}^5\text{Ni}^1\text{N}^1$ | 107.3517 |
| $\text{N}^2\text{--C}^1$ | 1.3276 | $\text{C}^9\text{N}^1\text{N}^2$ | 115.14 |
| $\text{N}^3\text{--C}^1$ | 1.3646 | $\text{C}^9\text{N}^1\text{Ni}^1$ | 131.03 |
| $\text{N}^3\text{--N}^4$ | 1.3576 | $\text{N}^2\text{N}^1\text{Ni}^1$ | 113.73 |
| $\text{N}^5\text{--N}^6$ | 1.3575 | $\text{C}^1\text{N}^2\text{N}^1$ | 111.74 |
| $\text{N}^7\text{--N}^8$ | 1.3585 | $\text{N}^4\text{N}^3\text{C}^1$ | 122.84 |
| $\text{N}^5\text{--C}^{31}$ | 1.3406 | $\text{N}^4\text{N}^3\text{Ni}^1$ | 124.13 |
| $\text{N}^6\text{--C}^{23}$ | 1.3296 | $\text{C}^1\text{N}^3\text{Ni}^1$ | 112.23 |
| $\text{N}^7\text{--C}^{23}$ | 1.3636 | $\text{C}^{31}\text{N}^5\text{N}^6$ | 116.14 |
| $\text{O}^1\text{--C}^{12}$ | 1.2276 | $\text{C}^{31}\text{N}^5\text{Ni}^1$ | 127.73 |
| $\text{O}^2\text{--C}^{34}$ | 1.2186 | $\text{N}^6\text{N}^5\text{Ni}^1$ | 115.53 |
| | | $\text{N}^8\text{N}^7\text{Ni}^1$ | 124.13 |

Waals radii], $\text{C}^{42}\text{--H}^{42B}\cdots\text{C}^{29ii}$, $d = 2.68 \text{ \AA}$ ($\delta = 0.22 \text{ \AA}$) [symmetry code (ii): $1 + x, y, z$].

In order to assess the relative stability of the possible isomeric forms of the complex **V** we carried out quantum-chemical calculation of the total energy of the *cis,trans*-isomers (singlet spin state) and high-spin (triplet spin state) isomers. Table 2 shows the total and relative energies of the isomers obtained in the framework of density functional theory (functional B3LYP) with the basis set 6-311G(d) (B3LYP column), Fig. 4, shows the optimal structures, Table 3 lists some of the geometric parameters.

The *trans*-isomer, as well as *cis*-isomer is not flat due to steric repulsion of quinonimine fragment of one ligand and phthalazine moiety of the second ligand. The angle between the least-mean-square planes of five-membered chelate rings is even more than in the *cis*-isomer, 42.7° .

In the high-spin isomer the ligand planes are turned by 73.4° , and the structure of coordination unit is close to the heavily distorted pseudotetrahedron, the N--Ni--N angles for the equivalent nitrogen atoms of the ligands are very different: 117.4° for $\text{N}^3\text{--Ni}^1\text{--N}^7$ and 160.3° for $\text{N}^1\text{--Ni}^1\text{--N}^5$.

The calculated optimal structure of the *cis*-isomer is close to the X-ray data, but there is a strong steric

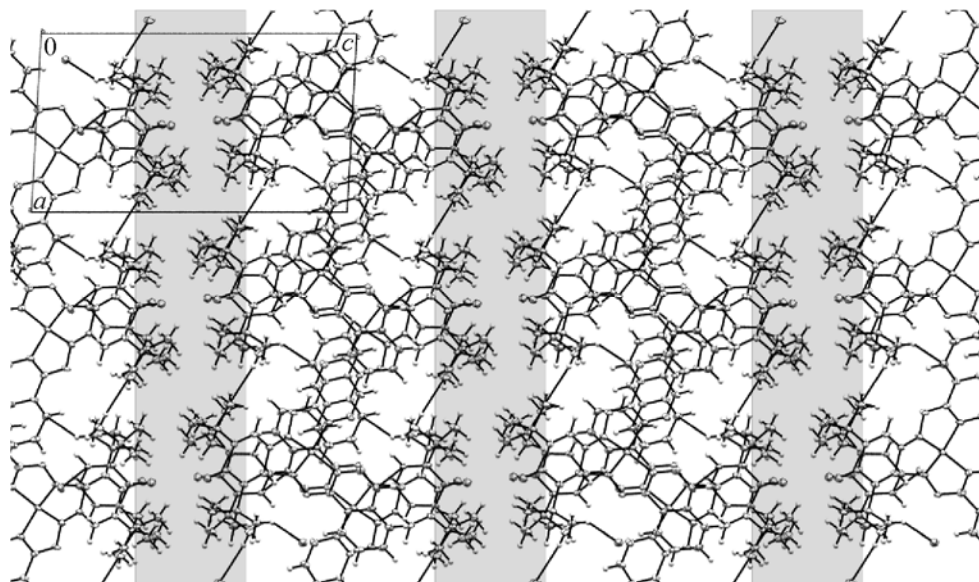


Fig. 3. The crystal packing of complex **V**, view along the crystallographic *b* axis. Darkened area corresponds to the hydrophobic interactions of *t*-butyl groups.

repulsion of the ligands, which is seen in the increased distances between atoms of quinonimine fragments of ligands in comparison with the data of X-ray diffraction (Table 3). Thus, the distance between the carbon atoms of quinonimine fragments C¹²–C³⁴ is overestimated by more than 1 Å.

As a result of the overestimation of the steric repulsion, the calculations with the B3LYP functional show that the *cis*-isomer of complex **V** is by 4.39 kcal mol^{–1} less stable than the *trans*-isomer. Furthermore, the *cis*-isomer is even less favourable than the high-spin isomers. This discrepancy between the results of calculations and experimental data can be explained by insufficient accounting for the nonbonded dispersion interaction between the ligands in the complex in the framework of DFT method. From the analysis of the crystal structure, however, the significant role of these interactions is obvious in the formation of supra-

molecular structure of the crystal. To account for the dispersion interaction between the ligands, we used the method of DFT-D3 proposed by Grimme and coworkers [41], in which the energy of the dispersion interaction is calculated as correction to the energy calculated by density functional theory (DFT)

$$E_{\text{DFT-D3}} = E_{\text{DFT}} - E_{\text{disp}}, \quad (1)$$

where E_{disp} is the sum of two-center contributions to the dispersion interaction. At short distances the Becke–Johnson damping function was applied [42–44].

Table 2 shows the results of calculation of the energy of isomers, Table 3 lists the optimum geometric parameters in the columns marked B3LYP-D3. Additional accounting for the dispersion correction has almost no effect on the bond lengths in the complex, but significantly improves the theoretical description of the equilibrium geometry of the interligand contacts

Table 2. Full (E , au) and relative (ΔE , kcal mol^{–1}) energies of isomers calculated using the methods of DFT (functional B3LYP) and B3LYP-D3

| Isomer | B3LYP | | B3LYP-D3 | |
|----------------|--------------|-------------------------------------|--------------|-------------------------------------|
| | E , au | ΔE , kcal mol ^{–1} | E , au | ΔE , kcal mol ^{–1} |
| <i>cis</i> - | –3802.506037 | 4.33 | –3802.783145 | 0.00 |
| <i>trans</i> - | –3802.512937 | 0.00 | –3802.782642 | 0.32 |
| Tetrahedral | –3802.509056 | 2.43 | –3802.776231 | 4.34 |

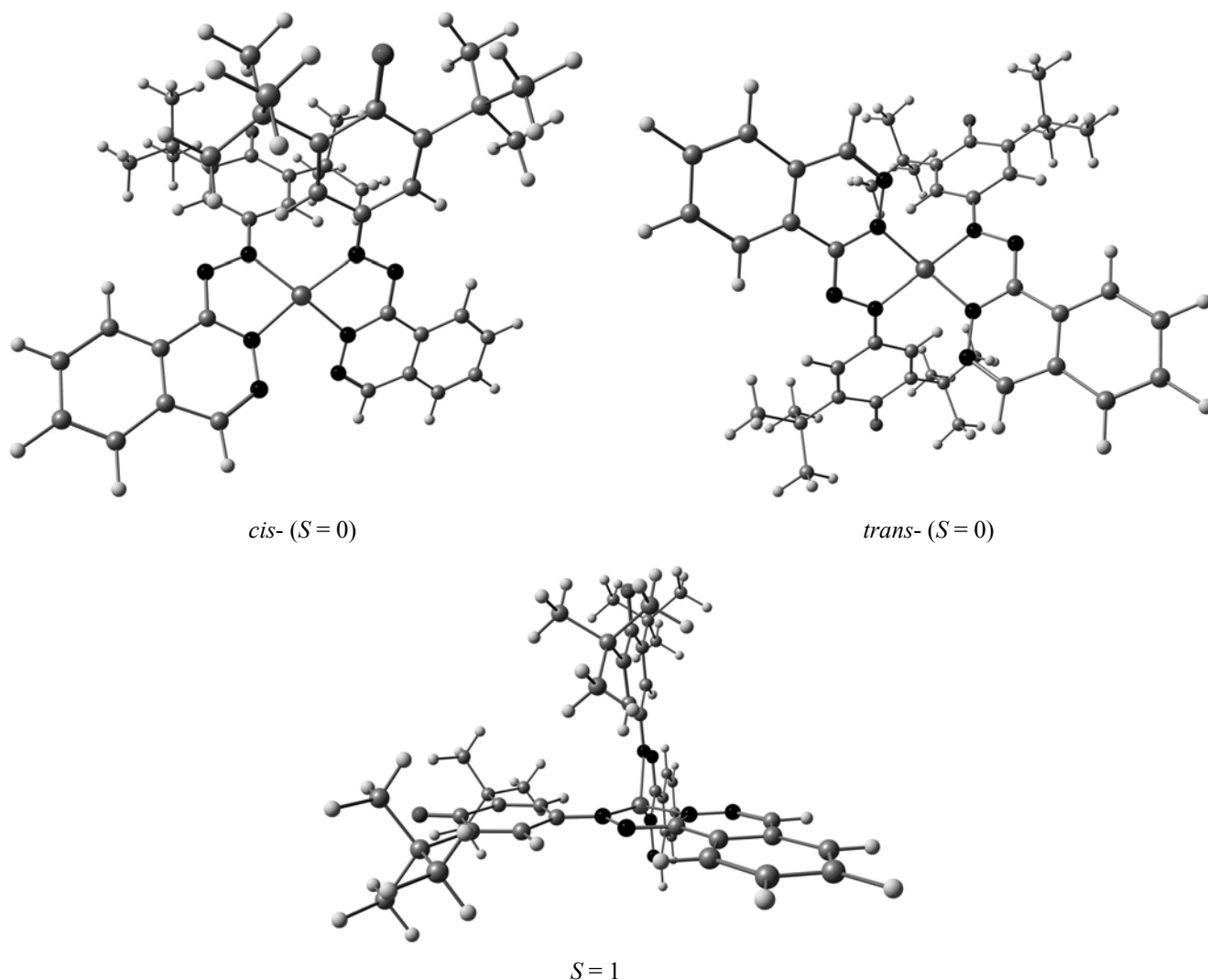


Fig. 4. Optimized low-spin *cis,trans*-structures ($S = 0$) and high-spin structure ($S = 1$) of complex **V** isomers.

in the complex, as can be seen by comparing the distances between the quinonimine substituents $C^{34}-C^{12}$, C^9-C^{31} , and $C^{14}-C^{36}$ of the ligands (Table 3). The improvement of description of steric repulsion between the ligands affects the decrease of the inflection angle in the five-membered chelate rings. Similar changes in the equilibrium geometry can be noted in the *trans*-isomer, but the relative stabilization of this isomer in the framework of DFT-D3 is much smaller. When taking into account the dispersion interaction, the *cis*-isomer becomes the most stable, by $0.3 \text{ kcal mol}^{-1}$ more stable than the *trans*-isomer.

Thus, the results of quantum chemical-calculations suggest that a key role in the stabilization of the *cis*-isomer of the complex **V** is the interligand dispersion interaction.

EXPERIMENTAL

^1H NMR spectra were taken from solutions in $\text{DMSO}-d_6$ on a Varian Unity 300 (300 MHz) spectrometer, internal reference HMDS. IR spectra were recorded on a Varian Scimitar spectrophotometer within $400\text{--}4000 \text{ cm}^{-1}$, samples were prepared as a suspension in mineral oil. The absorption spectra in the visible and ultraviolet regions were recorded on a Varian Cary 5000 spectrophotometer, solutions were investigated with a concentration of 10^{-3} M in toluene in cells 1 cm thick. Magnetic susceptibility was measured by Faraday method in the temperature range of $77.4\text{--}300 \text{ K}$.

Quantum-chemical calculations were performed in EC YUGINFO SFU cluster using Gaussian'03

Table 3. Selected geometric parameters (d , Å; angles, deg) for the optimal structures of *cis*- and *trans*-isomers of the complex **V** in the framework of B3LYP and B3LYP-D3 calculation compared to the XRD data for complex **V**

| Parameter | XRD ^a | B3LYP | | B3LYP-D3 | |
|--|------------------|------------|--------------|------------|--------------|
| | | <i>cis</i> | <i>trans</i> | <i>cis</i> | <i>trans</i> |
| $d(\text{Ni}^1\text{--N}^1)$, Å | 1.935 | 1.947 | 1.918 | 1.946 | 1.911 |
| $d(\text{Ni}^1\text{--N}^3)$, Å | 1.860 | 1.875 | 1.891 | 1.874 | 1.882 |
| $d(\text{N}^1\text{--N}^2)$, Å | 1.359 | 1.347 | 1.347 | 1.346 | 1.347 |
| $d(\text{N}^1\text{--C}^9)$, Å | 1.335 | 1.338 | 1.331 | 1.336 | 1.329 |
| $d(\text{N}^2\text{--C}^1)$, Å | 1.328 | 1.331 | 1.328 | 1.331 | 1.327 |
| $d(\text{N}^3\text{--C}^1)$, Å | 1.364 | 1.361 | 1.366 | 1.362 | 1.365 |
| $d(\text{N}^3\text{--N}^4)$, Å | 1.357 | 1.340 | 1.345 | 1.341 | 1.344 |
| Angle between the five-membered ring, deg | 38.8 | 38.3 | 42.7 | 36.0 | 39.0 |
| Inflection of the chelate ring at $\text{N}\cdots\text{N}$, deg | 4.2 and 8.9 | 12.8 | 17.6 | 10.8 | 13.2 |
| $d(\text{N}^1\text{--N}^5)$, Å | 3.117 | 3.133 | — | 3.111 | — |
| $d(\text{C}^9\text{--C}^{31})$, Å | 3.764 | 3.887 | — | 3.705 | — |
| $d(\text{C}^{12}\text{--C}^{34})$, Å | 5.470 | 6.601 | — | 5.304 | — |
| $d(\text{C}^{14}\text{--C}^{36})$, Å | 3.119 | 3.542 | — | 3.187 | — |

^a The mean values of the geometrical parameters for the two ligands in the complex are reported.

software [45]. To prepare the data, the presentation graphics, visualization of results of calculations we used the program Chemcraft [46].

Hydrazone (I). To a hot suspension of 0.391 g (2 mmol) of 1-hydrazinophthalazine hydrochloride in 20 mL of ethanol was added 0.164 g (2 mmol) of sodium acetate. The mixture was boiled for 10 min, 0.44 g (2 mmol) of 2,6-di-*tert*-butyl-*p*-quinone was added, and the reaction mixture was refluxed for 4 h. Then 50 mL of water was added and the mixture was left overnight. The orange precipitate was filtered off, washed with water and ethanol, and recrystallized from hexane. Yield 0.396 g (55%), mp 207°C. IR spectrum (ν , cm^{-1}): 3371 (NH), 1684 s (C=O), 1636 s, 1597 (C=N). ^1H NMR spectrum (CDCl_3 , δ , ppm): 10.928 s (1H, NH); 8.50–8.60 m (1H, CH_{arom}), 8.044 (1H, CH_{arom}), 7.70–7.80 m (2H, CH_{arom}), 7.56–7.67 m (1H, CH_{arom}) 8.094 d (1H, CH_{arom} , $J = 2.5$ Hz), 7.101 d (1H, CH_{arom} , $J = 2.5$ Hz), 1.328 s (9H, *t*-Bu); 1.356 s (9H, *t*-Bu). EAS in toluene (λ , nm): 471 (ϵ 34,500 $\text{L cm}^{-1} \text{mol}^{-1}$). Found, %: C 72.65, H 7.39, N 15.62. $\text{C}_{22}\text{H}_{26}\text{N}_4\text{O}$. Calculated, %: C 72.90, H 7.23, N 15.46.

Complexes II–V (general procedure). To a hot solution of 0.5 mmol of hydrazone **I** in 25 mL of methanol

was added a solution of 0.25 mmol of a metal acetate in 10 mL of methanol. The reaction mixture was refluxed for 30 min, the formed precipitate was filtered off, washed with methanol, and recrystallized from DMF.

Complex II. Yield 0.180 g (90%), mp > 250°C. IR spectrum (ν , cm^{-1}): 1672 s (C=O), 1619 s, 1594 (C=N). ^1H NMR spectrum (CDCl_3 , δ , ppm): 8.61–8.68 m (1H, CH_{arom}), 8.602 s (1H, CH_{arom}), 7.81–7.90 m (2H, CH_{arom}), 7.70–7.78 m (1H, CH_{arom}), 8.329 d (1H, CH_{arom} , $J = 2.6$ Hz), 6.584 d (1H, CH_{arom} , $J = 2.6$ Hz), 1.349 s (9H, *t*-Bu); 0.879 s (9H, *t*-Bu). EAS in toluene (λ , nm): 533 (ϵ 55,000 $\text{L cm}^{-1} \text{mol}^{-1}$). Found, %: C 67.25, H 6.30, N 14.03. $\text{C}_{44}\text{H}_{50}\text{N}_8\text{O}_2\text{Zn}$. Calculated, %: C 67.04, H 6.39, N 14.21.

Complex III. Yield 0.198 g (86%), mp > 250°C. IR spectrum (ν , cm^{-1}): 1677 s (C=O), 1622 s, 1592 (C=N). ^1H NMR spectrum (CDCl_3 , δ , ppm): 8.63–8.69 m (1H, CH_{arom}), 8.531 (1H, CH_{arom}), 7.78–7.89 m (2H, CH_{arom}), 7.65–7.73 m (1H, CH_{arom}), 8.178 d (1H, CH_{arom} , $J = 2.6$ Hz), 6.769 d (1H, CH_{arom} , $J = 2.6$ Hz), 1.318 s (9H, *t*-Bu); 0.869 s (9H, *t*-Bu). EAS in toluene (λ , nm): 527 (ϵ 67,000 $\text{L cm}^{-1} \text{mol}^{-1}$). Found, %: C 57.39, H 5.32, N 12.04. $\text{C}_{44}\text{H}_{50}\text{HgN}_8\text{O}_2$. Calculated, %: C 57.22, H 5.46, N 12.13.

Complex IV. Yield 0.177 g (90%), mp > 250°C. IR spectrum (ν , cm^{-1}): 1673 s (C=O), 1615 s, 1595 (C=N). EAS in toluene (λ , nm): 529 (ϵ 52,000 $\text{L cm}^{-1} \text{mol}^{-1}$). μ_{eff} (MB): 1.79 (300 K), 1.77 (77.4 K). Found, %: C 67.36, H 6.49, N 14.11. $\text{C}_{44}\text{H}_{50}\text{CuN}_8\text{O}_2$. Calculated, %: C 67.20, H 6.41, N 14.25.

Complex (V). Yield 0.176 g (90%), mp > 250°C. IR spectrum (ν , cm^{-1}): 1670 s (C=O), 1609 s, 1591 (C=N). ESP in toluene (nm): 474, 528 (ϵ 6200 $\text{L cm}^{-1} \text{mol}^{-1}$), 657. ^1H NMR spectrum (CDCl_3 , δ , ppm): 8.734 s (1H, CH_{arom}), 8.48–8.56 m (1H, CH_{arom}), 7.73–7.90 m (3H, CH_{arom}), 7.630 d (1H, CH_{arom} , $J = 2.8$ Hz), 7.373 d (1H, CH_{arom} , $J = 2.8$ Hz), 1.369 s (9H, *t*-Bu); 1.118 s (9H, *t*-Bu). Found, %: C 67.85, H 6.38, N 14.52. $\text{C}_{44}\text{H}_{50}\text{N}_8\text{NiO}_2$. Calculated, %: C 67.61, H 6.45, N 14.34.

A single crystal of the complex V for XRD was obtained by slow cooling of a solution in DMF. Dark green prismatic crystals ($M = 781.63$), triclinic at 100 K, $a = 9.696(5)$ Å, $b = 11.977(6)$ Å, $c = 17.393(9)$ Å, $\alpha = 100.654$ (10)°, $\beta = 91.963$ (10)°, $\gamma = 95.964$ (9)°, $V = 1971.4(17)$ Å³, space group *P1*, $Z = 2$, $\rho_{\text{calc}} = 1.317$ g cm⁻³. The intensities of 12,588 reflections were measured on a Bruker SMART APEX2 CCD diffractometer ($\lambda\text{Mo-}K_{\alpha} = 0.71073$ E, graphite monochromator, ω -scanning, $2\theta < 56^\circ$) for the single crystal of the size $0.21 \times 0.17 \times 0.14$ mm. Processing of the array of measured intensities was carried out by the program SAINT [47], SADABS [48]. The structure was solved by the direct method and refined (509 parameters) by full-matrix anisotropic approximation for non-hydrogen atoms with respect to F_{hkl}^2 . Hydrogen atoms were placed in geometrically calculated positions and refined using a *rider* model [$U_{\text{iso}}(\text{H}) = nU_{\text{eq}}(\text{C})$, where $n = 1.5$ for the carbon atoms of the methyl groups, $n = 1.2$ for the other C atoms]. In the refinement 9520 independent reflections were used. The refinement convergence $wR_2 = 0.1839$ (all reflections), $R_1 = 0.1465$ [7927 reflections with $I > 2\sigma(I)$]. All calculations were performed using the software package SHELXL-97 [49]. Atomic coordinates and temperature factors are deposited in the Cambridge Structural Database (CCDC 905945).

REFERENCES

1. Kitaev, Yu.P. and Buzykin, B.N., *Gidrazony* (Hydrazones), Moscow: Nauka, 1974.
2. Kogan, V.A., Zelentsov, V.V., Larin, G.M., and Lukov, V.V., *Kompleksy perekhodnykh metallov s gidrazonami. Fiziko-khimicheskie svoistva i stroenie* (Transition Metal Complexes with Hydrazones. Physical and Chemical Properties and Structure), Moscow: Nauka, 1990.
3. Parpiev, N.A., Yusupov, V.G., Yakimovich, S.I., and Sharipov, Kh.G., *Atsilgidrazony i ikh komplekсы s perekhodnymi metallami* (Acylhydrazones and Their Complexes with Transition Metals), Tashkent: Fan, 1988.
4. Stadler, A.-M. and Harrowfield, J., *Inorg. Chim. Acta.*, 2009, vol. 362, no. 12, p. 4298.
5. Popov, L.D., Morozov, A.N., Shcherbakov, I.N., Tupolova, Yu.P., Lukov, V.V., and Kogan, V.A., *Russ. Chem. Rev.*, 2009, vol. 78, no. 7, p. 643.
6. Kogan, V.A., Levchenkov, S.I., Popov, L.D., and Shcherbakov, I.N., *Russ. J. Gen. Chem.*, 2009, vol. 79, no. 12, p. 2767.
7. Zelenin, K.N., Khorseeva, L.A., and Alekseev, V.V., *Khim. Farm. Zh.*, 1992, vol. 26, no. 5, p. 30.
8. Vicini, P., Incerty, M., Doytchinova, I.A., La Colla, P., Busonera, B., and Loddo, R., *Eur. J. Med. Chem.*, 2006, vol. 48, no. 5, p. 624.
9. Budagumpi, S., Kulkarni, N.V., Sathisha, M.P., Netalkar, S.P., Revankar, V.K., and Suresh, D.K., *Monatsh. Chem.*, 2011, vol. 142, no. 5, p. 487.
10. Segura-Pacheco, B., Trejo-Becerril, C., Perez-Cardenas, E., Taja-Chayeb, L., Mariscal, I., Chavez, A., Acuna, C., Salazar, A.M., Lizano, M., and Duenas-Gonzalez, A., *Clinical Cancer Res.*, 2003, vol. 9, no. 5, p. 1596.
11. Arce, C., Segura-Pacheco, B., Perez-Cardenas, E., Taja-Chayeb, L., Candelaria, M., and Duennas-Gonzalez, A., *J. Transl. Med.*, 2006, vol. 4, no. 1, p. 10.
12. Kaminskas, L.M., Pyke, S.M., and Burcham, P.C., *J. Pharmacol. Exper. Therap.*, 2004, vol. 310, no. 3, p. 1003.
13. Kaminskas, L.M., Pyke, S.M., and Burcham, P.C., *Org. Biomol. Chem.*, 2004, vol. 2, no. 18, p. 2578.
14. Knowles, H.J., Tian, Y.M., Mole, D.R., and Harris, A.L., *Circ. Res.*, 2004, vol. 95, no. 2, p. 162.
15. Reece, P.A., *Med. Res. Rev.*, 1981, vol. 1, no. 1, p. 73.
16. Haegele, K.D., McLean, A.J., Du Souich, P., Barron, K., Laquer, J., McNay, J.L., Carrier, O., and Brit., *J. Clin. Pharmacol.*, 1978, vol. 5, no. 6, p. 489.
17. Nakashima, K., Shimada, K., and Akiyama, S., *Chem. Pharm. Bull.*, 1985, vol. 33, no. 4, p. 1515.
18. Razvi, T., Ramalingam, M., and Sattur, P.B., *Ind. J. Chem., Sect. B.*, 1989, vol. 28, no. 11, p. 987.
19. Giorgi, G., Ponticelli, F., Chiasserini, L., and Pellerano, C., *J. Chem. Soc., Perkin Trans. 2*, 2000, no. 11, p. 2259.
20. Odashima, T., Yamada, M., Yonemori, N., and Ishi, H., *Bull. Chem. Soc. Jpn.*, 1987, vol. 60, no. 9, p. 3225.
21. Paolucci, G., Stelluto, S., Sitran, S., Ajo, D., Benetollo, F., Polo, A., and Bombieri, G., *Inorg. Chim. Acta*, 1992, vol. 193, no. 1, p. 57.

22. Mochon, M.C., Gallego, M.C., and Perez, A.G., *Talanta*, 1986, vol. 33, no. 7, p. 627.
23. Mandal, S.K., Thompson, L.K., Newlands, M.J., Charland, J.-P., and Gabe, E.J., *Inorg. Chim. Acta*, 1990, vol. 178, no. 2, p. 169.
24. Shoukry, A.A. and Shoukry, M.M., *Spectrochim. Acta A*, 2008, vol. 70, no. 3, p. 686.
25. Popov, L.D., Shcherbakov, I.N., Levchenkov, S.I., Tupolova, Y.P., Kogan, V.A., and Lukov, V.V., *J. Coord. Chem.*, 2008, vol. 61, no. 3, p. 392.
26. Shcherbakov, I.N., Popov, L.D., Levchenkov, S.I., Morozov, A.N., Kogan, V.A., and Vikrishchuk, A.D., *Russ. J. Gen. Chem.*, 2009, vol. 79, no. 4, p. 826.
27. Popov, L.D., Levchenkov, S.I., Shcherbakov, I.N., Tupolova, Yu.P., Zubenko, A.A., Melkozerova, I.E., Lukov, V.V., and Kogan, V.A., *Russ. J. Gen. Chem.*, 2010, vol. 80, no. 9, p. 1853.
28. Popov, L.D., Levchenkov, S.I., Shcherbakov, I.N., Kogan, V.A., and Tupolova, Yu.P., *Russ. J. Gen. Chem.*, 2010, vol. 80, no. 3, p. 493.
29. Popov, L.D., Levchenkov, S.I., Shcherbakov, I.N., Minin, V.V., Tupolova, Yu.P., Zubenko, A.A., and Kogan, V.A., *Russ. J. Gen. Chem.*, 2010, vol. 80, no. 12, p. 2501.
30. Popov, L.D., Shcherbakov, I.N., Levchenkov, S.I., Tupolova, Yu.P., Burlov, A.S., Aleksandrov, G.G., Lukov, V.V., and Kogan, V.A., *Russ. J. Coord. Chem.*, 2011, vol. 37, no. 7, p. 483.
31. Butcher, R.J., Jasinski, J.P., Yathirajan, H.S., Vijesh, A.M., and Narayana, B., *Acta Cryst. E*, 2007, vol. 63, no. 9, p. o3674.
32. Büyükgüngör, O., Odabasoglu, M., Vijesh, A.M., and Yathirajan, H.S., *Acta Cryst. E*, 2007, vol. 63, no. 10, p. o4084.
33. Popov, L.D., Levchenkov, S.I., Shcherbakov, I.N., Starikova, Z.A., Kaimakan, E.B., and Lukov, V.V., *Russ. J. Gen. Chem.*, 2012, vol. 82, no. 3, p. 465.
34. Stephens, P.J., Devlin, F.J., Chabalowski, C.F., and Frisch, M.J., *J. Phys. Chem.*, 1994, vol. 98, no. 45, p. 11623.
35. Becke, A.D., *J. Chem. Phys.*, 1993, vol. 98, no. 7, p. 5648.
36. Lee, C., Yang, W., and Parr, R.G., *Phys. Rev., B*, 1988, vol. 37, no. 2, p. 785.
37. Rakitin, Yu.V. and Kalinnikov, V.T., *Sovremennaya magnetokhimiya* (Modern Magnetochemistry), St. Petersburg: Nauka, 1994.
38. Kahn, O., *Molecular Magnetism*, New York: VCH Publishers, 1993.
39. Kogan, V.A., Lyubchenko, S.N., Shcherbakov, I.N., Ionov, A.M., Tkachev, V.V., Shilov, G.V., and Aldoshin, S.M., *Russ. J. Coord. Chem.*, 2005, vol. 31, no. 8, p. 533.
40. Kogan, V.A. and Shcherbakov, I.N., *Russ. Khim. Zh.*, 2004, vol. 48, no. 1, p. 69.
41. Grimme, S., Antony, J., Ehrlich, S., and Krieg, H., *J. Chem. Phys.*, 2010, vol. 132, no. 15, p. 154104.
42. Johnson, E.R. and Becke, A.D., *J. Chem. Phys.*, 2005, vol. 123, no. 2, p. 024101.
43. Johnson, E.R. and Becke, A.D., *J. Chem. Phys.*, 2006, vol. 124, no. 17, p. 174104.
44. Grimme, S., Ehrlich, S., and Goerigk, L., *J. Comput. Chem.*, 2011, vol. 32, no. 7, p. 1456.
45. Frisch, M.J., Trucks, G.W., Schlegel, H.B., Scuseria, G.E., Robb, M.A., Cheeseman, J.R., Montgomery, J.A., Jr., Vreven, T., Kudin, K.N., Burant, J.C., Millam, J.M., Iyengar, S.S., Tomasi, J., Barone, V., Mennucci, B., Cossi, M., Scalmani, G., Rega, N., Petersson, G.A., Nakatsuji, H., Hada, M., Ehara, M., Toyota, K., Fukuda, R., Hasegawa, J., Ishida, M., Nakajima, T., Honda, Y., Kitao, O., Nakai, H., Klene, M., Li, X., Knox, J.E., Hratchian, H.P., Cross, J.B., Bakken, V., Adamo, C., Jaramillo, J., Gomperts, R., Stratmann, R.E., Yazyev, O., Austin, A.J., Cammi, R., Pomelli, C., Ochterski, J.W., Ayala, P.Y., Morokuma, K., Voth, G.A., Salvador, P., Dannenberg, J.J., Zakrzewski, V.G., Dapprich, S., Daniels, A.D., Strain, M.C., Farkas, O., Malick, D.K., Rabuck, A.D., Raghavachari, K., Foresman, J.B., Ortiz, J.V., Cui, Q., Baboul, A.G., Clifford, S., Cioslowski, J., Stefanov, B.B., Liu, G., Liashenko, A., Piskorz, P., Komaromi, I., Martin, R.L., Fox, D.J., Keith, T., Al-Laham, M.A., Peng, C.Y., Nanayakkara, A., Challacombe, M., Gill, P.M.W., Johnson, B., Chen, W., Wong, M.W., Gonzalez, C., and Pople, J.A., *Gaussian 03*, Revision, D.01, Gaussian, Inc., Wallingford CT, 2004.
46. Zhurko, G.A., *Chemcraft ver. 1.6 (build 338)*. <http://www.chemcraftprog.com>.
47. SMART and SAINT, Release 5.0, *Area Detector Control and Integration Software*, Bruker AXS, Analytical X-Ray Instruments, Madison, Wisconsin, USA, 1998.
48. Sheldrick, G.M., *SADABS: A Program for Exploiting the Redundancy of Area-Detector X-Ray Data*, Göttingen: Univ. of Göttingen, Germany, 1999.
49. Sheldrick, G.M., *Acta Cryst. A*, 2008, vol. 64, no. 1, p. 112.